Multilayer-Induced Reaction of Cyclobutane on Ir(111): Identification of Reaction Products and Quantification of Reaction Kinetics†

Christopher J. Hagedorn,*,‡ Michael J. Weiss,‡ and W. Henry Weinberg‡,§

Department of Chemical Engineering, University of California at Santa Barbara, Santa Barbara, California 93106-5080, and Department of Chemistry, University of California at Santa Barbara, Santa Barbara, California 93106-9510

Received: July 6, 2000; In Final Form: January 3, 2001

We have studied the low temperature adsorption of cyclobutane on the hexagonally close-packed (hcp) Ir(111) surface using temperature-programmed desorption (TPD) and high-resolution electron energy loss spectroscopy (HREELS). Monolayer and submonolayer cyclobutane coverages desorb essentially completely in TPD experiments, whereas in the presence of a condensed cyclobutane multilayer, significant reaction of first-layer cyclobutane is observed. Based on the HREELS and TPD measurements, a C_4H_8 metallacycle is believed to be the predominate reaction intermediate that is formed in the initial reaction step during multilayer-induced reaction (MIR) of cyclobutane on Ir(111). The TPD spectra suggest that MIR of cyclobutane on Ir(111) results in three different reaction products: (1) surface carbon and hydrogen adatoms formed via complete decomposition of cyclobutane, (2) desorption of *n*-butane, and (3) desorption of 1-butene. Moreover, the extent of MIR has been quantified and is used in conjunction with a kinetic model in order to quantify the kinetics of the MIR of cyclobutane on this surface. The MIR kinetics are well described by a rate expression which is first order in the coverage of unreacted cyclobutane and the rate coefficient of which can be expressed in Polanyi−Wigner form with a preexponential factor of $k_r^{(0)} = 6.4 \times 10^{13}$ s^{-1} and an activation energy of $E_r = 8\,500 \pm 700$ cal/mol. This value represents a significant decrease in the activation barrier for reaction of cyclobutane on Ir(111) compared to the value of 10 270 cal/mol recently measured for the trapping-mediated dissociative chemisorption of cyclobutane on this same surface in the submonolayer regime at low temperature (300−400 K). This activation barrier reduction for MIR of cyclobutane on Ir(111) is qualitatively similar to that observed recently for the MIR of cyclobutane on Ru(001). The potential implications of these results toward providing a better understanding of catalytic reactions that occur at the solid−liquid interface are discussed.

I. Introduction

For decades, scientists have placed much emphasis on understanding gas-phase and liquid-phase heterogeneously catalyzed reactions. While considerable data exist for both gas−solid and liquid−solid catalytic reactions, little is known regarding the mechanistic link between these two areas of heterogeneous catalysis. For catalytic reactions at the gas−solid interface, ultrahigh vacuum (UHV) studies on well-defined surfaces have yielded significant information regarding the reaction mechanisms of industrially important heterogeneously catalyzed reactions.[1−3] Relatively little, however, has been reported for catalytic reactions at the interface between a liquid and a single-crystalline surface. The difficulty of maintaining a liquid on a surface under UHV conditions is, in part, responsible for this gap. Normally, high partial pressures or extremely low surface temperatures are required to keep a condensed phase on the surface. However, the presence of high partial pressures of a reactant gas makes maintaining surface cleanliness difficult and also precludes the use of electron spectroscopies that are successfully used to investigate heterogeneous reactions at the gas−solid interface. In the present study, cryogenic temperatures are used to maintain a condensed layer of cyclobutane on the Ir(111) surface to facilitate the study of reactions which occur in the presence of a condensed phase on a well-defined catalytic surface.

Our previous experimental studies concerning the adsorption of cyclobutane on the Ru(001) surface at 90 K showed conclusively that the presence of a condensed cyclobutane multilayer enhanced the rate of reaction of first layer molecular cyclobutane.[4,5] For submonolayer coverages of cyclobutane on Ru(001), adsorption is associative, as judged by HREELS and TPD measurements. Only a negligible amount of cyclobutane decomposition was observed for submonolayer coverages and was assigned to dissociation at highly reactive surface defect sites.[6] As the cyclobutane exposure was increased to the condensed multilayer regime, significant reaction of monolayer cyclobutane occurred, resulting in two different reaction products.[7,8] Carbon and hydrogen adatoms, produced by the complete decomposition of cyclobutane on the surface was the primary reaction product, while the other reaction product, which desorbed from the surface at a temperature of 200 K, was tentatively identified as 1-butene. The overall extent of reaction, determined by summing the fractional coverages of carbon adatoms participating in the formation of each reaction product, increased nearly linearly with multilayer coverage for the range of initial cyclobutane exposures investigated.

† Part of the special issue "John T. Yates, Jr. Festschrift".

* Corresponding Author. E-mail: chris_hagedorn@mckinsey.com.
‡ Department of Chemical Engineering.
§ Department of Chemistry.

10.1021/jp0024221 CCC: $20.00
Published on Web 04/10/2001

More recently, we have presented a model that was used to quantify the kinetic parameters associated with the enhanced rate of reaction of cyclobutane on Ru(001) due to the presence of a condensed multilayer.[9] The activation barrier and preexponential factor which describe the MIR of cyclobutane on Ru(001) were found to be 7 510 cal/mol and 5.0×10^{10} s^{-1}, respectively. The MIR activation barrier is significantly lower than that measured for trapping-mediated dissociative chemisorption of cyclobutane on the clean Ru(001) surface of 10 090 cal/mol.[5] The significant activation barrier decrease in the presence of a condensed phase has potentially important implications for our understanding of heterogeneously catalyzed reactions that occur at the liquid−solid interface. Because of the great potential of these recent findings in developing an understanding of heterogeneously catalyzed reactions at the liquid−solid interface, we have extended our study of MIR to include the reaction of cyclobutane with the Ir(111) surface. Our goals in the present study are 4-fold: (1) to report the observation of MIR of cyclobutane on Ir(111), (2) to identify the MIR pathways and MIR products of cyclobutane on Ir(111), (3) to quantify the kinetics of MIR of cyclobutane on Ir(111), and (4) to compare the MIR of cyclobutane on Ir(111) with the MIR already reported for cyclobutane on Ru(001) in the hope of developing a better understanding of reactions that occur at the liquid−solid interface.

II. Experimental Methodologies

The experiments were carried out in a stainless steel ultrahigh vacuum (UHV) chamber (base pressure of 7×10^{-11} Torr) equipped with HREELS, Auger electron spectroscopy (AES), low-energy electron diffraction (LEED), X-ray photoelectron spectroscopy (XPS), a twice differentially pumped radical beam source, and a differentially pumped quadrupole mass spectrometer for TPD measurements.[10−12] The HREEL spectra were acquired using a commercial LK-2000 HREEL spectrometer (LK Technologies) the resolution of which varied between 50 and 70 cm^{-1} (full width at half-maximum of the elastically scattered beam) while maintaining a counting rate of at least 5×10^4 Hz in the elastically scattered peak in the specular direction.

The Ir(111) single-crystal sample was mounted on a home-built cryostat that can cool the sample to 90 K using liquid nitrogen. The temperature of the crystal could be varied from 90 to 1700 K by resistive heating; the sample temperature was monitored using a type-C thermocouple that was spot-welded to the back of the crystal. The surface was cleaned using standard methods of Ar^+ sputtering as well as annealing to 1100 K in a background of oxygen. To remove all chemisorbed oxygen,[13] the crystal was heated to 1450 K; surface cleanliness was verified by HREELS, LEED, carbon monoxide TPD, and AES. The sample temperature was always kept below 800 K except in the presence of adsorbed oxygen in order to prevent the formation of graphite on the surface.

Cyclobutane and cyclobutane-d_8 reagents were synthesized via Wurtz coupling[14] reactions as described elsewhere[5] and were purified to greater than 99% purity by performing several freeze−pump−thaw cycles. The 1-butene (99+%) and *n*-butane (99.5%) hydrocarbons used for cracking fragment identification were obtained from Aldrich (Milwaukee) and Matheson Gas (New Jersey), respectively. All of the experiments performed in this study began with the adsorption of cyclobutane on the clean Ir(111) surface at 90 K. Cyclobutane exposures between 0.35 and 50.0 L (1 Langmuir (L) = 1×10^{-6} Torr s) were obtained by continuously flowing cyclobutane into the UHV chamber at pressures between 1×10^{-8} and 1×10^{-7} Torr (uncorrected for ion gauge sensitivity) for times ranging between 35 and 500 s. Immediately following each cyclobutane exposure, a TPD measurement was performed starting at a surface temperature of 90 K and ending at a temperature of 800 K. The sample was then allowed to cool to below 100 K, after which a TPD experiment was performed in the presence of a background pressure of 1×10^{-7} Torr of O_2. This procedure resulted in the production of reaction-limited CO that was formed by the reaction of oxygen with carbon adatoms present on the surface as a result of the decomposition of molecular cyclobutane during the multilayer-induced reaction. Using this method, no CO_2 was detected, and background adsorption of CO onto the surface during exposure of the oxygen was found to be negligible. The coverage of carbon adatoms deposited on the surface due to multilayer-induced decomposition of cyclobutane, $\theta_{C,s}$ (number of carbon atoms per surface iridium atom), was calculated by comparing the time-integrated area of the reaction-limited CO desorption in each experiment to the desorption of a saturation coverage of CO on Ir(111) of $\theta_{CO,sat} = 0.71$.[15]

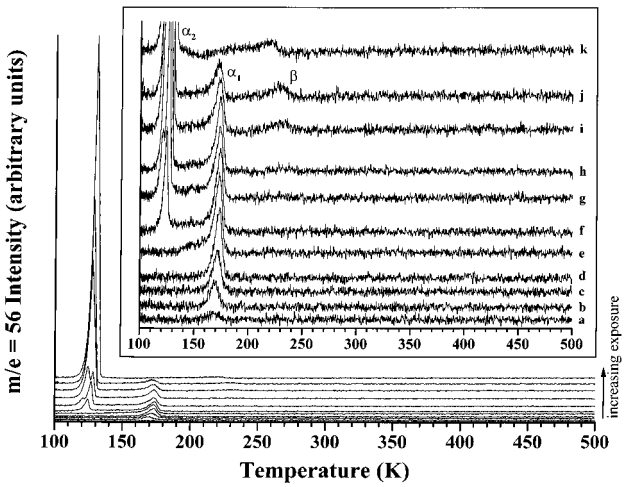

Figure 1. TPD spectra of $m/e = 56$ (c-C_4H_8) collected after exposure of the clean Ir(111) surface at 90 K to cyclobutane exposures of (in Langmuir (L)): (a) 0.35, (b) 0.7, (c) 1.0, (d) 1.5, (e) 2.0, (f) 3.5, (g) 5.0, (h) 8.5, (i) 17.0, (j) 25.5, and (k) 50.0. The heating rate for all spectra is 3.2 K/s.

III. Results and Discussion

A. Cyclobutane Thermal Desorption. The TPD spectra of cyclobutane ($m/e = 56$), collected for various initial exposures of c-C_4H_8 onto the Ir(111) surface at a temperature of 90 K, are displayed in Figure 1. A single desorption peak, labeled α_1, is observed at approximately 170 K for low c-C_4H_8 exposures; α_1 is attributed to first-order molecular desorption of monolayer cyclobutane from the Ir(111) surface. The activation energy for desorption of the α_1 peak was calculated to be $E_d = 10\,300 \pm 50$ cal/mol using the method of Redhead[16] assuming a preexponential factor for desorption of $k_d^{(0)} = 1 \times 10^{13}$. The intensity of the α_1 peak increases with increasing exposure until it saturates at an exposure of approximately 2 L. Once the α_1 peak saturates, a second desorption peak labeled α_2 is observed. The α_2 peak, which is assigned to zeroth-order multilayer (in this manuscript multilayer is defined as the second and higher adsorbed layers) desorption of molecular cyclobutane, increases monotonically in intensity with increasing initial cyclobutane exposure. The desorption of cyclobutane from the Ir(111) surface in two distinct desorption peaks is almost

identical to that reported previously for the desorption of cyclobutane from Ru(001).[4,5] The decreasing intensity and slight downshift in temperature of the α_1 monolayer desorption peak for exposures greater than 2.0 L are also nearly identical to observations made in these previous studies on Ru(001). Since a much larger fraction of the α_1 cyclobutane monolayer is reacting (and thus not desorbing) in the presence of a condensed multilayer than the negligible amount that would have reacted without the presence of a condensed multilayer, it is clear that MIR of cyclobutane on Ir(111) occurs. This type of decomposition would not be surprising if the trailing edge of the multilayer desorption peak were located at a temperature higher than the α_1 desorption temperature, thereby pinning the monolayer cyclobutane adsorbates on the surface above the α_1 desorption temperature. However, since even the highest multilayer coverages used here have left the surface by 135 K, at least an initial reaction step in the MIR of monolayer cyclobutane has already occurred by 135 K.

A third $m/e = 56$ desorption peak, labeled β, is observed at a temperature of approximately 230 K for initial cyclobutane exposures greater than 5.0 L. The β desorption peak intensity increases monotonically with increasing cyclobutane exposure up to the 50.0 L maximum exposure studied here. At an exposure of 50.0 L, the β desorption peak downshifts in temperature, broadens to even lower temperature, and becomes convoluted with the α_1 monolayer desorption peak. An estimate of the relative contributions of the α_1 and β peaks to the integrated area of the broad peak observed between 150 and 230 K in Figure 1(k) results in fractional contributions of 0.20 and 0.80, respectively, for α_1 and β. Since the β peak intensity increases with increasing initial exposure concomitant with a decrease in the α_1 monolayer cyclobutane peak, it seems likely that the β peak cannot be attributed to molecular cyclobutane desorption. Therefore, additional TPD experiments were performed at an initial cyclobutane exposure of 25.5 L (Figure 1(j)) in order to monitor other cracking fragments besides $m/e = 56$.

As expected, these multiplexed TPD experiments showed conclusively that both the α_1 and α_2 desorption peaks arise from desorption of molecular cyclobutane. The cracking fragments observed for the β desorption peak, however, are strikingly different from those observed for the α_1 and α_2 desorption peaks. Displayed in Figure 2A are the TPD spectra of the four most intense cracking fragments of the β desorption peak (m/e = 41, 43, 27, and 56, respectively) and the highest m/e ratio for which a signal was observed ($m/e = 58$) for the β desorption peak. The Figure 2B column chart displays the maximum intensities for each of these β cracking fragments, normalized so that the most intense cracking fragment, $m/e = 41$, has an intensity of unity. Since the normalized maximum intensities and normalized integrated TPD intensities of the cracking fragments are essentially the same here due to the nearly identical shapes and positions of the β desorption cracking fragment peaks, maximum intensities are used here. Also included in Figure 2B are the corresponding intensities observed for the α cyclobutane desorption peaks for each of these m/e ratios; the intensities of the α cracking fragments are also normalized to have an $m/e = 41$ cracking fragment intensity of unity. The most striking difference between the cracking fragments of the α and β desorption peaks is the absence of a $m/e = 43$ signal for the α peaks and the presence of a strong $m/e = 43$ signal for the β desorption peak. Another important observation from Figure 2B is the presence of a $m/e = 58$ cracking fragment for the β desorption product. On the basis of these data, the conclusion can easily be made that the β desorption product cannot be assigned as molecular cyclobutane. Therefore, mass spectral data tables[17] were employed as a means of identifying possible hydrocarbon molecules with cracking fragment patterns similar to the β desorption product.

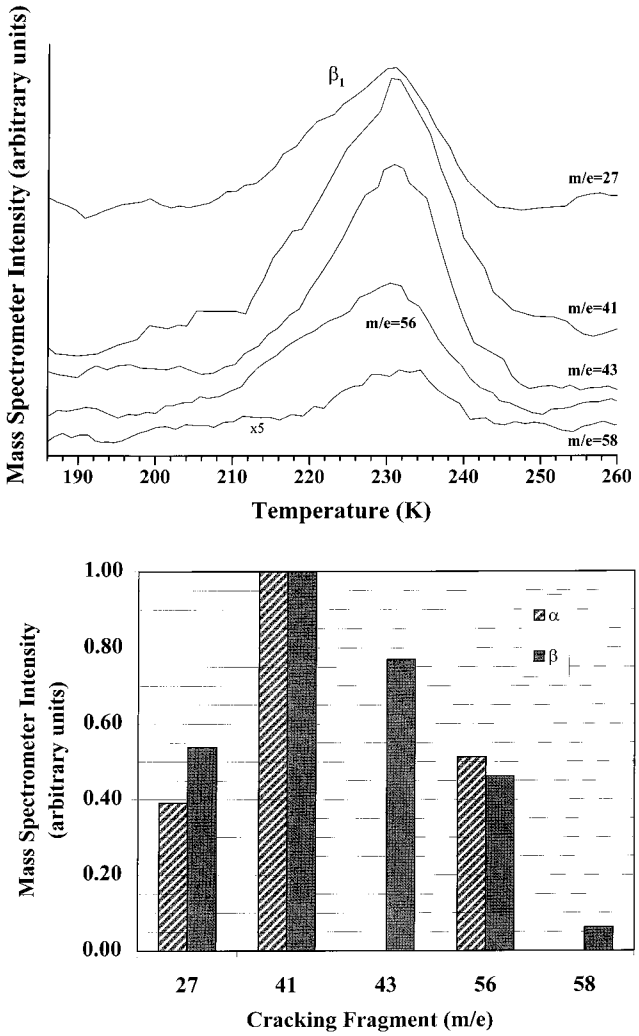

Figure 2. (A). TPD spectra of selected m/e signals of the β desorption product for an initial c-C_4H_8 exposure of 25.5 L (Figure 1(j)). The spectra displayed are the four with the most intense signals, $m/e = 41$, 43, 27, and 56, and the one with the highest m/e ratio, $m/e = 58$, for which a signal was observed. (B). Relative intensities of the β desorption product cracking pattern displayed in Figure 2A. The intensities of the cyclobutane α desorption product cracking pattern are displayed for comparison. The intensities are normalized so that the $m/e = 41$ cracking fragment intensities are equal to unity.

B. Identification of MIR Products. Since $m/e = 58$ is the highest m/e ratio observed for the β desorption product, the search for a hydrocarbon molecule with a cracking pattern similar to that reported here for the β desorption product was focused primarily on molecules containing four carbon atoms (C_4). Since the balance of such a molecule contains only hydrogen, hydrocarbons with m/e values between 48 and 58 were examined as the prime candidates. However, in the search for a hydrocarbon molecule with the proper cracking pattern, the full range of hydrocarbons between C_1 and C_8 was examined. The most closely matching hydrocarbon species were those of larger (C_4-C_8) partially branched hydrocarbons. Although some promising candidates contained some of the major β cracking fragments, no single C_1-C_8 hydrocarbon molecule could provide a good fit to the observed experimental data due to at least one *major* disparity between the reported cracking pattern

and the pattern observed here for the β desorption peak. Therefore, a linear combination of the cracking patterns of two different hydrocarbon species was considered as a possible fit to the β desorption product cracking fragmentation data.

Since α cyclobutane is a C_4 hydrocarbon, and the cracking fragment with the highest m/e ratio ($m/e = 58$) observed for the β desorption product also must be a C_4 hydrocarbon, it seems reasonable to focus the search to linear combinations of C_4 hydrocarbons. Excluding the possibility of hydrocarbon reaction products greater than C_4, that would be formed via C−C bond formation reactions on this surface, is also reasonable based on the literature.[18−23] For example, high-pressure experiments involving the hydrogenation, isomerization, and hydrogenolysis of cyclopropane, methylcyclopropane, and propylene (0.4 to 10 Torr) in the presence of hydrogen (20 to 500 Torr) on Ir(111) and Ir(110)-(1 × 2) surfaces resulted in the observation of some active C−C bond cleavage reaction pathways; however, no evidence for any C−C bond coupling reactions[19] was observed. The dehydrogenation of C_3 hydrocarbons propane, cyclopropane, propylene, propyne, and allene on the Ir(110)-(1 × 2) surface was reported to proceed through a common intermediate of approximate stoichiometry C_3H_2 with no evidence of any C−C bond coupling reactions.[20] For the reactions of ethane, propane, isobutane, and neopentane with the Ir(110)-(1 × 2) surface, no hydrocarbons other than those initially adsorbed were found to desorb from the surface.[21] Finally, adsorption of ethylene on Ir(111) is believed to result in decomposition to ethylidyne by a temperature of 180 K.[22,23] The ethylidyne moiety decomposes further to C_2H fragments at approximately 300 K; no evidence for C−C bond coupling is observed for the interaction of ethylene with Ir(111). In summary, no C−C bond coupling reactions have been observed in these studies involving hydrocarbons (some of which are very similar to cyclobutane) on well-defined iridium surfaces, even under more harsh high-pressure and high-temperature conditions[19] than used in this present study. Therefore, limiting the search to a linear combination of C_4 hydrocarbons is warranted based on the literature.

Recently, we have provided strong experimental evidence in support of formation of a C_4 reaction product from cyclobutane; 1-butene was observed as a reaction product via both trapping-mediated dissociative chemisorption and MIR pathways for the reaction of cyclobutane on Ru(001).[7,8] The 1-butene reaction product desorption temperature of 200 K reported on Ru(001) is very similar to that observed here for the β desorption product. Therefore, butene, and more specifically, 1-butene, appears to be a good choice for use in linear combination with other C_4 hydrocarbons in the attempt to describe the cracking pattern of the β desorption product. Because the $m/e = 58$ cracking fragment is the β desorption product cracking fragment with the highest m/e ratio, it is probable that this is the molecular parent ion of one of the β desorption products. The only two choices of C_4 hydrocarbon molecules with $m/e = 58$ containing only carbon and hydrogen are *n*-butane and isobutane. However, since formation of isobutane from cyclobutane requires isomerization via formation of a C−C bond (and only after cleavage of two cyclobutane C−C bonds), the possibility that isobutane is formed on the surface is highly unlikely. Therefore the arguments presented thus far suggest that *n*-butane and 1-butene are the two most obvious choices for use in linear combination in the attempt to identify the β desorption product.

Although mass spectral data tables[17] were used initially to confirm that *n*-butane and 1-butene were possible cracking pattern matches, slight differences in mass spectrometer operating parameters can cause slight differences in the relative intensities of cracking patterns. Therefore, to obtain the most accurate quantitative cracking pattern data from *n*-butane and 1-butene, the background mass spectrum of each hydrocarbon was recorded in our system using the same spectrometer that was used to record the β desorption product cracking pattern. Displayed in Figure 3 are the cracking patterns of *n*-butane and 1-butene collected using the mass spectrometer located in the UHV chamber. It is important to note that the total background pressure of each molecule in the chamber during collection of these spectra was precisely identical; this will be essential in the calculation of the relative contributions of *n*-butane and 1-butene in the β desorption peak. No ionization gauge correction factors were required here since the absolute ionization gauge sensitivities for butane and butene are the same within experimental error.[24]

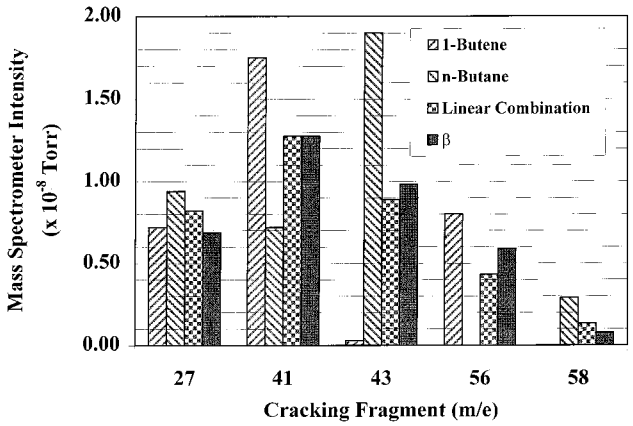

Figure 3. Comparison of the cracking patterns for *n*-butane, 1-butene, a linear combination of 0.46 *n*-butane, and 0.54 1-butene, and the β desorption product. The individual m/e ratio mass spectrometer intensities for *n*-butane and 1-butene are absolute values as determined by introducing equal pressures into the UHV chamber. The β desorption product cracking pattern intensities are normalized for easy comparison so that the most abundant cracking fragment, $m/e = 41$, has an intensity identical to that reported for the $m/e = 41$ cracking fragment from the linear combination.

As can be seen in Figure 3, the cracking patterns of *n*-butane and 1-butene at the same background pressure are notably different, especially when comparing the measured intensities for the $m/e = 41$ and 43 cracking fragments. The linear combinations of cracking patterns displayed in Figure 3 were calculated using the expression $I_{lc,i} = \eta I_{n-\text{butane},i} + (1 - \eta) I_{1-\text{butene},i}$, where $I_{lc,i}$ is the intensity of the linear combination m/e ratio i, $I_{n-\text{butane},i}$ is the intensity of the *n*-butane m/e ratio i, $I_{1-\text{butene},i}$ is the intensity of the 1-butene m/e ratio i, and η is the fraction of *n*-butane in the linear combination calculation. This relation only holds true and returns an accurate value for the fraction of each hydrocarbon in the mixture if the two reference cracking patterns are collected at precisely the same background pressure. The linear combination cracking pattern in Figure 3, calculated with a value of $\eta = 0.46$, results in a cracking pattern which very closely matches the (normalized) cracking pattern for the β desorption product. The value of η was optimized by minimizing the summation of the squares of the differences between the β desorption peak cracking fragment intensities and the cracking fragment intensities calculated using the linear combination expression. It should be noted here that the optimal fit procedure used to determine η was also a function of the normalization factor used for the β desorption product cracking pattern. Coincidentally, the optimal normalization factor results in equal peaks intensities for both the $m/e = 41$ β desorption

peak and the $m/e = 41$ linear combination cracking fragment. The value of η which resulted in the best fit to the experimental data was $\eta = 0.46 \pm 0.05$. The quoted error represents one standard deviation in the value of η and was estimated by taking into account the standard deviations of the measured intensities of each cracking fragment for *n*-butane, 1-butene, and the β desorption peak.

While this analysis provides an extremely good fit to the cracking pattern data for the β desorption product, one must use caution in stating absolutely that this linear combination of *n*-butane and 1-butene is the correct identification of the β desorption product. For instance, it is certainly true that other C_4 hydrocarbon molecules such as 2-butene and isobutane can provide reasonable fits to the β desorption peak cracking pattern data when substituted for 1-butene and *n*-butane, respectively. Also, it is possible that higher carbon number ($>C_4$) hydrocarbons are contributing to the β desorption peak, but go unnoticed because their molecular ions and larger *m*/*e* ratio cracking fragments are fairly weak in intensity. However, as has already been discussed above, reaction mechanisms requiring formation of C−C bonds seem highly unlikely since C−C bond formation is not observed for other hydrocarbons on iridium surfaces. Therefore, if we rule out hydrocarbon molecules with greater than four carbon atoms and isobutane on the basis of these arguments, it seems likely that *n*-butane is one component of the β desorption product. The arguments in favor of 1-butene as compared to the other C_4 hydrocarbons which have a large $m/e = 56$ intensity are not as definitive. Since the other component (besides *n*-butane) must have a large $m/e = 56$ intensity, and most likely must be a C_4 hydrocarbon, the only possibilities that fit this description are butene isomers (isobutene, 1-butene, *cis*-2-butene, and *trans*-2-butene). Isobutene can be ruled out based on the same C−C bond formation arguments that allowed us to rule out isobutane as a substitute for *n*-butane. The other three butene isomers have nearly identical cracking patterns,[17] making absolute assignment of the exact butene isomer present in the β desorption product difficult. We will again discuss this difficult issue of the assignment of a butene isomer in the context of the HREELS data and reaction mechanism discussions below. Not being able to identify conclusively a single linear butene isomer, however, will not impede our efforts in quantifying the extent of reaction. Similar linear combination analyses performed for *cis*-2-butene and *trans*-2-butene resulted in values for η which fell within the quoted error bars. As will be shown in the next section, quantification of the average ratio of hydrogen atoms to carbon atoms in the β desorption product will be extremely important in the quantification of the extent of MIR. However, since η does not vary appreciably by substituting the different linear butene isomers for 1-butene in linear combination with *n*-butane, the average ratio of hydrogen atoms to carbons atoms in the β desorption product will not vary appreciably either.

Now that tentative identification of the β desorption product as a combination of nearly equal fractions of *n*-butane and 1-butene has been made, discussion of possible reaction mechanisms is possible. Since the *n*-butane and 1-butene β products desorb from the surface at essentially the same temperature, the reaction mechanisms for both *n*-butane and 1-butene formation most likely have the same rate-limiting step.[25] Also, because the desorption temperature of *n*-butane from the clean Ir(111) surface is approximately 180 K,[26] the rate-limiting step in the desorption of the *n*-butane β product from the surface at 230 K most likely cannot be the desorption step itself, but rather, a reaction step. Based on these observations, it is likely that formation and subsequent desorption of *n*-butane and 1-butene share the same rate-limiting reaction step.

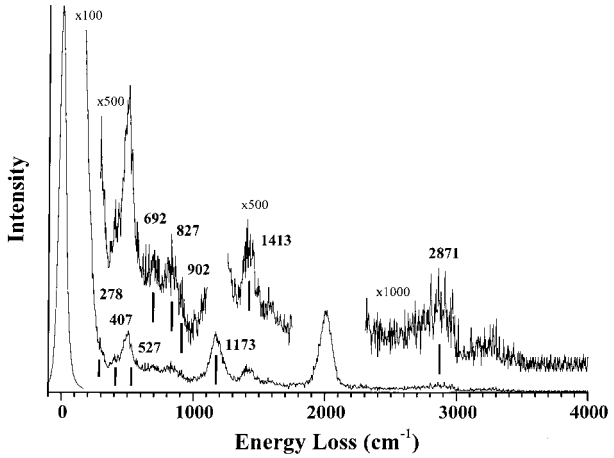

Figure 4. Specular direction HREELS spectrum collected immediately after halting the thermal desorption experiment in Figure 1(j) at a temperature of 200 K.

Since the first step in the reaction of cyclobutane with the surface must be either cleavage of a C−C or a C−H bond, the initial reaction intermediate is likely to be either a C_4H_8 metallacycle or a C_4H_7 cyclobutyl group. To identify the reaction intermediate present on the surface after the initial dissociation step, HREELS data were collected immediately after stopping the TPD experiment shown in Figure 1(j) at a temperature of 200 K. The HREEL spectrum is displayed in Figure 4; mode assignments and selected peaks from relevant reference compounds are displayed in Table 1. Examination of the tentative vibrational assignments listed in Table 1 reveals that the modes observed here at a surface temperature of 200 K are consistent with the presence of a C_4H_8 metallacycle intermediate. The vibrational spectrum for bromocyclobutane, useful as a reference compound for a surface-bound cyclobutyl, has a few features in common with the modes observed in Figure 4. However, the lack of a mode at 1262 cm^{-1} corresponding to the strong bromocyclobutane β CH_2 wag [27, 28] suggests that cyclobutyl groups are not present in any significant concentration on the surface. Therefore, for the experimental conditions used here, the vibrational data suggest that the predominate initial dissociation pathway for MIR of cyclobutane on Ir(111) occurs via initial C−C bond cleavage to form a C_4H_8 metallacycle intermediate.

The two weak modes, present in the HREEL spectrum of Figure 4 at 1586 and 3240 cm^{-1}, suggest the presence of a small coverage of hydrocarbon moieties having carbon atoms with a combination of sp and sp^2 hybridization. The interaction of a C═C bond with the hydrocarbon modified surface may cause a slight rehybridization of the C═C bond, which would cause the C═C frequency to downshift below 1600 cm^{-1}. The rather high frequency of the C−H stretching mode could possibly be explained by repulsive steric interactions of the hydrogen atom with adjacent hydrocarbon moieties. Nothing definitive can be said about these two modes, however, since they could also be attributed to a slight amount of background water adsorption during HREELS acquisition.[29] The vibrational features centered at 496 and 2007 cm^{-1} are most likely due to background adsorption of CO during HREELS acquisition.[30] The additional vibrational features present in Figure 4 can possibly be attributed to C_4 reaction intermediates formed from the subsequent reaction of the C_4H_8 metallacycle below 200 K. Reference compound vibrational assignments for *n*-butyl (1-iodobutane) and 3-butenyl

TABLE 1: HREELS Mode Assignments for a 25.5 L Exposure of c-C_4H_8 on Ir(111) Annealed to 200 K[a]

approximate mode description	25.5 L c-C_4H_8 200 K/Ir(111)	C_4H_8 metallacycle c-C_4H_8 MIR/Ru(001)[b]	approximate mode description	1-iodobutane (20 K)[c]	1-butene (77 K)[d]	bromo-cyclobutane[e]
frustrated translation	278(sh)	238	C−X stretch + CCC bend	593		301, 486
CH_2 rock	692		CH_2 rock	735, 778		701
ring deformation	527	550	α C−H deformation			824
CC stretch, ring deformation	827, 902(sh)	922	CC stretch + CH_2 rock	864	836	
CC stretch + CH_2 wag/twist	1173(b)	1160, 1309	CH_2 rock/twist	897		
CH_2 scissor	1413	1412	ring stretch			1016
CH stretch	2871(b)	2796, 2884	CC stretch + CH_2 twist	1190	1128	
			β CH_2 wag			1262
			CH_2 scissor	1427	1414, 1436	
			CH_3 bend	1451		
			C=C stretch		1638	
			CH stretch	2840−3008	2884−3079	2856−2996
			2(C=C stretch)		3270	

[a] All vibrational modes are in cm^{-1}; selected vibrational modes from relevant reference compounds are also listed. w = weak, sh = shoulder, b = broad. [b] Reference 8. [c] References 28, 39−41. [d] References 28, 42. [e] References 27, 28.

(1-butene) moieties are displayed in Table 1. The relevance of these particular reference compounds will become clear in the discussion below.

Since the vibrational data suggest that the predominant reaction pathway for the MIR of cyclobutane on Ir(111) occurs via initial C−C bond cleavage, resulting in the formation of a C_4H_8 metallacycle, discussion of the possible reaction pathways which lead to the desorption of both *n*-butane and 1-butene from this metallacycle intermediate is possible. Recall from the discussion above that the rate-limiting steps for the formation of *n*-butane and 1-butene are most likely identical. Since the presumed initial MIR step to form a C_4H_8 metallacycle via initial C−C bond cleavage occurs below 135 K, and the β desorption product does not desorb until above 200 K, the initial C−C bond cleavage step cannot be the rate-limiting step in the formation of *n*-butane and 1-butene. For the formation of *n*-butane from the C_4H_8 metallacycle, the most plausible reaction pathway involves hydrogenation of one end of the di-σ-bonded radical C_4H_8 to form an *n*-butyl moiety, followed by subsequent hydrogenation of the *n*-butyl moiety to *n*-butane product (which immediately desorbs). Other reaction pathways for formation of *n*-butane from the C_4H_8 metallacycle can, of course, be proposed, but none would be as straightforward as the two-step hydrogenation of the metallacycle to *n*-butane. Any other reaction pathways leading to *n*-butane formation would have to include a hydrogenolysis or dehydrogenation step. However, since these mechanisms would require additional bond formation reactions to occur to form *n*-butane after the bond dissociation reactions, such mechanisms would seem to be energetically and entropically disfavored. Therefore, we feel that the most likely reaction pathway for the formation of *n*-butane from the C_4H_8 metallacycle involves a two-step hydrogenation. We will show that this reaction pathway provides the greatest possibility of sharing a rate-limiting reaction step with the reaction pathway for formation of 1-butene.

If the formation of *n*-butane proceeds via the two-step hydrogenation pathway, then there would appear to be only two plausible reaction pathways for the formation of 1-butene that could result in similar rate-limiting steps. The first possible 1-butene formation reaction pathway would involve the formation of an *n*-butyl moiety via hydrogenation of the C_4H_8 metallacycle intermediate, followed by β-hydride elimination of the *n*-butyl moiety to form the 1-butene desorption product (Scheme 1). In this case, the *identical* rate-limiting step of hydrogenation of the C_4H_8 metallacycle to an *n*-butyl moiety would be shared. The second proposed reaction pathway for formation of 1-butene involves the formation of a 3-butenyl moiety via β-hydride elimination of the C_4H_8 metallacycle, followed by hydrogenation of the 3-butenyl moiety to form the 1-butene product (Scheme 2). In this case, the *similar* rate-limiting steps for the formation of the *n*-butane and 1-butene desorption products would involve hydrogenation of the *n*-butyl and 3-butenyl moieties, respectively. One can imagine that it is possible for the difference between the initial and transition states for both the *n*-butyl and 3-butenyl hydrogenation reactions to be nearly identical, thereby resulting in similar kinetics. However, it seems unlikely that both reactions would have *precisely* the same *difference* between initial and transition state geometries necessary for the two reactions to occur at almost exactly the same temperature. Therefore, the most likely reaction pathway for the production of *n*-butane and 1-butene by the MIR of cyclobutane on Ir(111) appears to be Scheme 1.

SCHEME 1: Reaction Scheme Depicting Possible Reaction Pathways for MIR of Cyclobutane on Ir(111) Which Share the Identical Rate-Limiting Step for the Formation of Both *n*-Butane and 1-Butene β Desorption Product

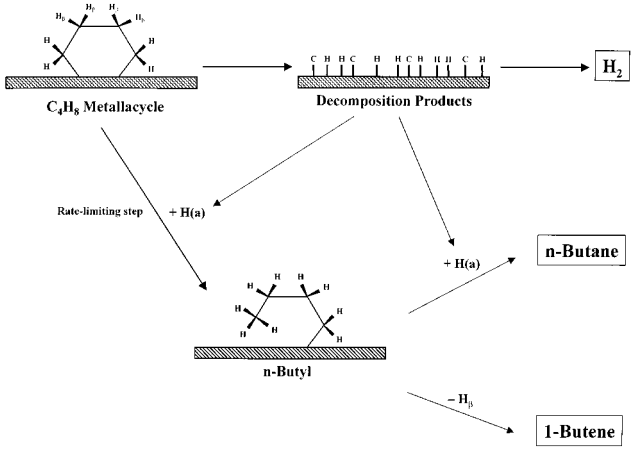

Scheme 1 also seems to be more plausible than Scheme 2 when considering that the proportion of *n*-butane and 1-butene in the β desorption product did not appear to change with initial cyclobutane exposure (and, therefore, extent of reaction). It might be expected that reaction pathways which share fewer identical reaction steps may result in β desorption product compositions which change with variations in the initial

SCHEME 2: Reaction Scheme Depicting Possible Reaction Pathways for MIR of Cyclobutane on Ir(111) Which Have a Similar Rate-Limiting Step for the Formation of *n*-Butane and 1-Butene β Desorption Product

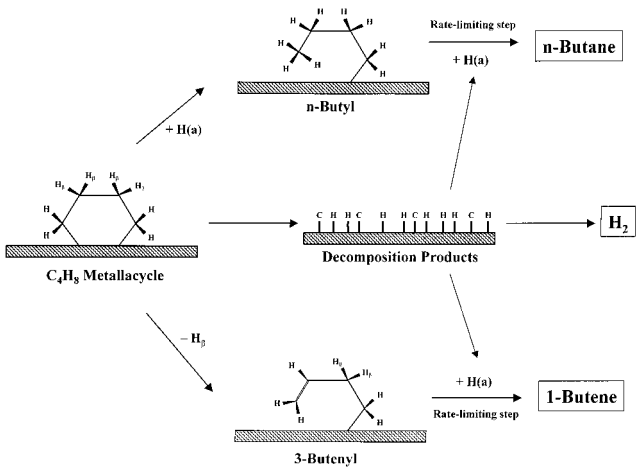

cyclobutane exposure because of reaction rate coefficients for the different reaction steps which change differently with surface coverage. Reaction pathways that share identical reaction pathways through the rate-limiting elementary step would be expected to yield approximately the same β desorption product compositions since the rates of reaction for production of both *n*-butane and 1-butene should be equal. A final point concerning the HREELS data and possible reaction schemes should be mentioned. The vibrational data suggest the possibility that a moderate amount of *n*-butyl moieties could be present on the surface at 200 K (the onset of desorption of the β product), as evidenced by the strong vibrational feature at 1173 cm^{-1}. Although this suggests the possible presence of *n*-butyl moieties on the surface immediately prior to desorption of the β product, no definitive choice of one reaction scheme over the other can be based on this observation.

The tentative spectroscopic identification of a surface metallacycle as the initial reaction intermediate, combined with TPD results and mechanistic arguments suggesting that the formation of both *n*-butane and 1-butene desorption products likely proceeds via identical rate-limiting steps, enables us to propose that the MIR of cyclobutane on Ir(111) occurs via reaction Scheme 1. Under these experimental conditions, it appears that a majority of the cyclobutane molecules that react via MIR initially react via C−C bond cleavage to form a C_4H_8 metallacycle. Since the multilayer induces this reaction, this initial reaction step must occur below 135 K. The initial metallacycle reaction intermediate then likely undergoes rate-limiting hydrogenation to form *n*-butyl, followed by either fast hydrogenation to form *n*-butane or fast β-hydride elimination to form 1-butene. During the thermal desorption measurements, a portion of the cyclobutane also undergoes complete decomposition to carbon and hydrogen adatoms, the latter of which are partially consumed in the hydrogenation reactions to form *n*-butane. Sufficient evidence is not available to identify the reaction intermediates involved in the complete decomposition of cyclobutane to surface carbon and hydrogen adatoms; therefore, we will not speculate on the possible mechanisms and intermediates for this reaction pathway. However, the carbon adatoms left on the surface after decomposition via this reaction pathway have been quantified and will be discussed below.

C. Quantification of Multilayer-Induced Extent of Reaction. To quantify the MIR kinetics for cyclobutane on Ir(111), it is first necessary to quantify the extent of reaction as a function of initial cyclobutane exposure. The definition of extent of reaction used here simply refers to the amount of monolayer cyclobutane that reacts with the surface. The extent of reaction will be quantified as the fractional coverage of total carbon atoms, $\theta_{C,tot}$, that react via MIR of cyclobutane. Immediately before performing the cyclobutane TPD experiments on Ir(111), the entire fractional coverage of carbon atoms that eventually react via MIR are all in the form of physically adsorbed cyclobutane. However, as the surface is heated in the TPD experiments, a portion of the physically adsorbed cyclobutane monolayer reacts via MIR.

Based on the discussion presented above, the MIR of cyclobutane on Ir(111) is believed to result in the production of three different reaction products as shown in Scheme 1: decomposition of cyclobutane leading to the deposition of surface carbon and hydrogen adatoms, the formation of *n*-butane β desorption product, and the formation of 1-butene β desorption product. To quantify the kinetics of MIR of cyclobutane on this surface, it is essential that the extent of reaction, $\theta_{C,tot}$, is calculated as a function of initial cyclobutane exposure. Quantification of $\theta_{C,tot}$ requires performing mass balance calculations on the fractional coverage of carbon atoms and hydrogen atoms that are involved in the MIR. The two mass balance equations governing the fractional coverage of carbon and hydrogen are

$$\theta_{C,tot} = \theta_{C,s} + \theta_{C,dp} \quad (1)$$

$$\theta_{H,tot} = \theta_{H,s} + \theta_{H,dp} \quad (2)$$

where $\theta_{C,s}$ and $\theta_{H,s}$ are the fractional coverages of carbon and hydrogen adatoms left on the surface following decomposition of cyclobutane, $\theta_{C,dp}$ and $\theta_{H,dp}$ are the fractional coverages of carbon and hydrogen atoms that leave the surface as β desorption product, and $\theta_{C,tot}$ and $\theta_{H,tot}$ are the fractional coverages of carbon and hydrogen atoms originally present in the fraction of cyclobutane molecules that react via MIR. Two more equations can be written relating the ratio of hydrogen atoms to carbon atoms in both the initial cyclobutane reactant and β desorption product. By definition, the relationship between $\theta_{C,tot}$ and $\theta_{H,tot}$ can be written as

$$\theta_{H,tot} = 2\theta_{C,tot} \quad (3)$$

since the initial cyclobutane reactant has a hydrogen atom to carbon atom ratio of 2 to 1. Using the previously calculated fractions of 0.46 *n*-butane and 0.54 1-butene found to be present in the β desorption product, the calculated hydrogen atom to carbon atom ratio present in the β desorption product is 2.23 to 1, enabling the following expression to be written:

$$\theta_{H,dp} = 2.23\theta_{C,dp} \quad (4)$$

As already mentioned above, this ratio is fairly robust in that even if the C_4 desorption products were slightly different than the *n*-butane and 1-butene assignments previously made, i.e., isobutane and *trans*-2-butene, this ratio would still be approximately the same due to the fact that one butane and one butene isomer would have to be used in order to achieve a reasonable fit to the β desorption cracking pattern. Within the detectability limits of our mass spectrometer, no change in the β desorption cracking pattern was observed as a function of initial cyclobutane exposure; therefore, the ratio of 2.23 remains constant for all initial cyclobutane exposures.

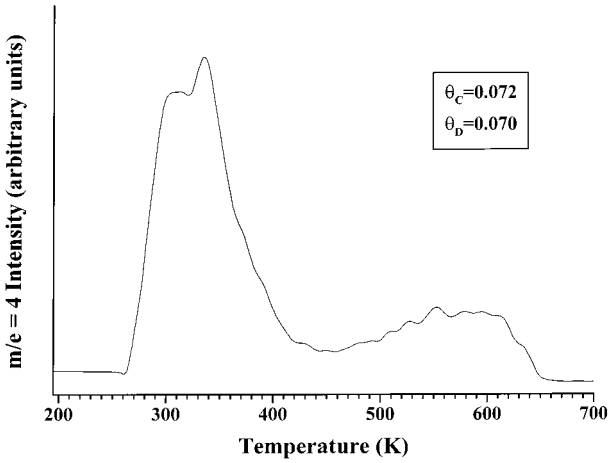

Figure 5. TPD of recombinative D_2 ($m/e = 4$) desorption following exposure of the Ir(111) surface at 90 K to 25.5 L of c-C_4D_8. The surface coverage of carbon adatoms left on the surface (due to decomposition of cyclobutane) following the D_2 desorption is $\theta_C = 0.072$. The heating rate was 3.2 K/s.

Now that four equations have been written with six total unknowns, only two additional degrees of freedom must be removed in order to find a closed solution for the extent of reaction $\theta_{C,tot}$. If we examine the TPD spectrum displayed in Figure 5 showing recombinative desorption of D_2 resulting from the reaction pathway leading to decomposition of cyclobutane into carbon and deuterium adatoms on the surface for an initial c-C_4D_8 exposure of 25.5 L, $\theta_{H,s}$ can be calculated at this initial exposure. By comparing the time-integrated intensity of the D_2 thermal desorption in Figure 5 with that obtained for a saturation coverage of deuterium adatoms, $\theta_{D,sat} = 1.0$, produced via dissociative chemisorption of D_2 on Ir(111),[31,32] $\theta_{H,s}$ is calculated to be 0.070 for an initial cyclobutane exposure of 25.5. L. Although c-C_4D_8 was used here to more accurately quantify $\theta_{H,s}$ since D_2 TPD spectra are much better resolved than H_2 TPD spectra in the UHV chamber, no isotope effect was observed that would cause the value for $\theta_{H,s}$ to be different for c-C_4H_8. It should be mentioned that $\theta_{H,s}$ remains relatively constant over the entire range of initial cyclobutane exposures studied here. Next, by performing the oxygen titration procedure described in the Experimental Section of this manuscript, we were able to quantify the surface coverage of carbon adatoms left on the surface, $\theta_{C,s}$, following multilayer-induced decomposition of cyclobutane. For an initial cyclobutane exposure of 25.5 L, a value of $\theta_{C,s} = 0.072$ is measured. From eqs 1−4 and the values of $\theta_{C,s} = 0.072$ and $\theta_{H,s} = 0.070$ determined for an initial cyclobutane exposure of 25.5 L, the extent of reaction, $\theta_{C,tot}$, can now be calculated at an initial exposure of 25.5 L. The calculated value for the extent of reaction at an initial cyclobutane exposure of 25.5 L is $\theta_{C,tot} = 0.39$. Now that all variables displayed in eqs 1,2 have been quantified for an initial cyclobutane exposure of 25.5 L, a proportionality constant, S_β, can be calculated which relates the time-integrated area of the β desorption peak, A_β, to the fractional coverage of the β desorption product, $\theta_{C,dp}$. This relationship is given by $\theta_{C,dp} = S_\beta A_\beta$. Using this proportionality factor and the A_β values for each initial exposure, $\theta_{C,dp}$ was calculated for each initial cyclobutane exposure. The oxygen titration experiments were performed after the TPD experiments for each initial exposure in order to calculate $\theta_{C,s}$ as a function of initial cyclobutane exposure. Finally, the extent of reaction, $\theta_{C,tot}$, was calculated as a function of initial cyclobutane exposure by simply summing the values of $\theta_{C,dp}$ and $\theta_{C,s}$, cf., eq 1.

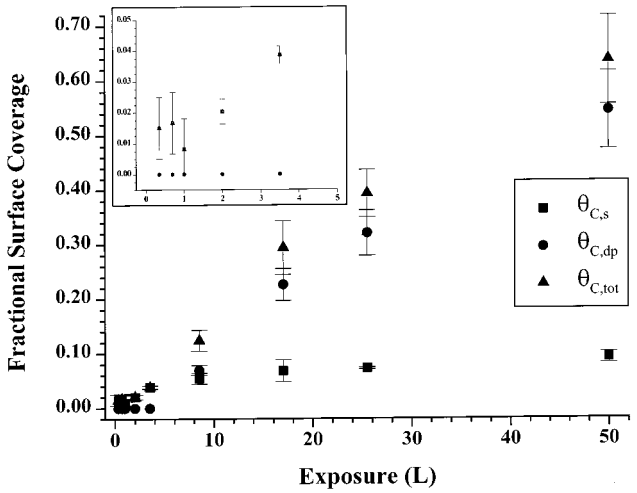

Figure 6. Fractional surface coverage of carbon atoms as a function of initial c-C_4H_8 exposure. Surface carbon adatoms remaining following decomposition of c-C_4H_8 to surface carbon adatoms and hydrogen adatoms (which desorb as H_2) are labeled as $\theta_{C,s}$. Carbon atoms that desorb from the surface as β desorption product following reaction of c-C_4H_8 to form the β product are labeled as $\theta_{C,dp}$. The third series in the figure, $\theta_{C,tot} = \theta_{C,s} + \theta_{C,dp}$, is the total fractional coverage of carbon adatoms (present initially on the surface as molecular c-C_4H_8) that react via multilayer-induced reaction during the interaction of c-C_4H_8 with the Ir(111) surface. The inset shows an expanded view of the data for exposures between 0 and 5 L. The error bars represent one standard deviation in the measured value at each exposure.

Displayed in Figure 6 are the values of $\theta_{C,s}$, $\theta_{C,dp}$, and $\theta_{C,tot}$ as a function of initial cyclobutane exposure. For initial exposures below 2 L, the extent of reaction remains relatively constant at a value of $\theta_{C,tot} \approx 0.015$; this small, relatively constant extent of reaction over the entire range of submonolayer coverages is most likely due to the irreversible decomposition of monolayer cyclobutane molecules at highly reactive surface defect sites.[4,6] As the initial exposure is increased to the multilayer coverage regime (exposures > 2 L), the extent of reaction increases dramatically with exposure and continues to increase nearly linearly with cyclobutane exposure for the range of exposures studied here. Since exposures of approximately 3.5 L and below yield no β desorption product, the dominant reaction pathway for MIR of cyclobutane for this range of initial exposures is decomposition of cyclobutane to surface carbon adatoms. For initial cyclobutane exposures above 3.5 L, the multilayer-induced β desorption product reaction pathway becomes active and dominates the overall extent of reaction. The relatively large error bars on the $\theta_{C,tot}$ values are a result of the propagated errors associated with the composition determination of the β desorption product and the random errors associated with the measured thermal desorption integrated intensities.

D. Quantification of Multilayer-Induced Reaction Kinetics. Now that the extent of reaction has been quantified as a function of initial cyclobutane exposure, kinetic parameters that describe the MIR can be extracted from the experimental data by fitting the MIR model proposed by Weiss, et al.[9] to the experimental data. Two different MIR models were proposed in this previous work. One of the models incorporates a Heaviside function that immediately "turns off" the MIR channel once the multilayer has completely desorbed from the surface. The other model, which was shown to be the more accurate model in the previous work, includes a second layer coverage factor which slowly "turns off" the MIR channel as the second cyclobutane layer desorbs from the surface in the trailing edge

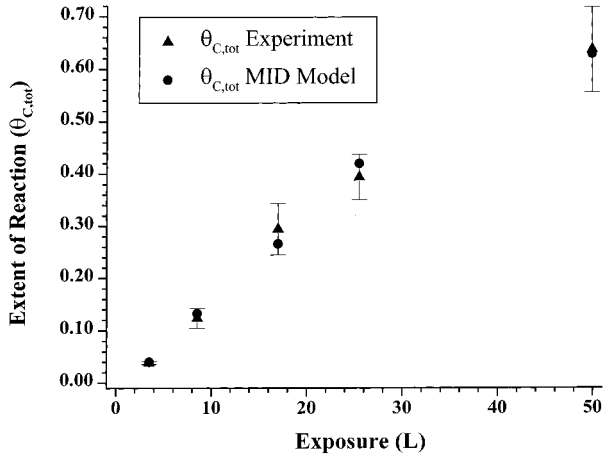

Figure 7. Comparison of the experimentally determined extent of reaction, $\theta_{C,tot}$, with the calculated values from the multilayer-induced reaction model as a function of initial c-C_4H_8 exposure. The error bars represent one standard deviation in the measured value at each exposure.

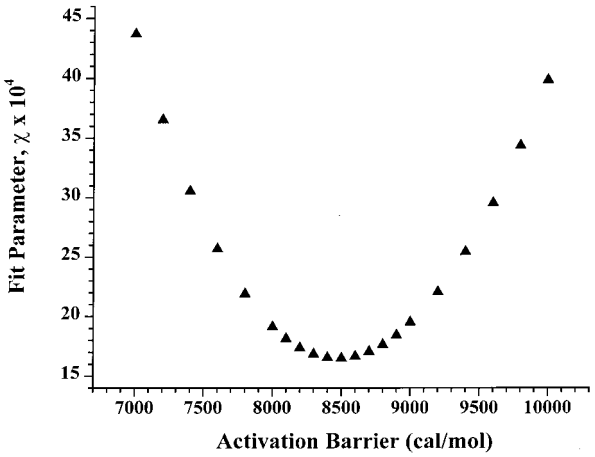

Figure 8. Fit parameter, χ, the summation of the squares of the differences between the multilayer-induced reaction model and the experimental extent-of-reaction data, displayed as a function of activation barrier used in the multilayer-induced reaction model.

of the multilayer desorption peak. The model including the second layer coverage term will be used here to extract the kinetic parameters describing MIR of cyclobutane on Ir(111). In the model, the rate of MIR, r, is given by

$$r = k_r^{(0)} \exp(-E_r/k_B T)\theta_{C,CB}\theta_{C,2nd\ layer} \qquad (5)$$

where $k_r^{(0)}$ is the preexponential factor and E_r is the activation barrier for MIR, k_B is the Boltzmann constant, T is the surface temperature, $\theta_{C,CB}$ is the fractional coverage of carbon atoms present in molecular cyclobutane in the monolayer, and $\theta_{C,2nd\ layer}$ is the coverage of carbon atoms present in cyclobutane in the second cyclobutane layer. The $\theta_{C,2nd\ layer}$ coverage factor has a value of unity until the last stages of multilayer desorption, where it then decreases gradually to a value of zero as the second layer of cyclobutane desorbs from the surface in the trailing edge of the multilayer desorption peak. We assume here that the saturation concentration of cyclobutane present in the first and second layers is the same.

The experimental values for the extent of reaction are displayed in Figure 7 along with the calculated values using the MIR model in connection with eq 5. Only initial cyclobutane exposures greater than 2.0 L were included in Figure 7 since a multilayer is not present to induce reaction for initial exposures of 2.0 L or lower. The best-fit kinetic parameters were determined by minimizing the goodness of fit, χ, which is defined as the summation of the squares of the differences between the experimental and predicted values of $\theta_{C,tot}$. The procedure for finding the best-fit kinetic parameters involved choosing an activation barrier and then varying the preexponential factor in order to find the minimum value of χ for that activation barrier. This procedure was performed for a large range of activation barriers; the best-fit activation barrier and preexponential factor were the pair of kinetic parameters that yielded a minimum value for χ. A plot of χ versus activation barrier is provided in Figure 8; clearly the activation barrier providing the best fit to the experimental data is $E_r = 8\ 500$ cal/mol. The accompanying preexponential factor used to obtain the best-fit activation barrier of $E_r = 8\ 500$ cal/mol is $k_r^{(0)} = 6.4 \times 10^{13}\ s^{-1}$.

Considering all of the quoted errors associated with the calculation of the extent of reaction, we estimate the uncertainty of the activation barrier to be approximately ± 700 cal/mol. Because the preexponential factor must compensate greatly for changes in the activation barrier, the approximate error for the preexponential factor is estimated to be plus-or-minus 1 order of magnitude. It should be mentioned here that although the error bar values for $\theta_{C,dp}$ are quite large, and dominate the error values quoted for $\theta_{C,tot}$ due to the propagated errors from the determination of the β desorption product composition, these errors are of a systematic nature and thus cause the entire range of $\theta_{C,tot}$ values to shift in a concerted manner within the error bar range. Such a concerted shift in all of the extent of reaction values in either the positive or negative direction, although relatively large, would result in the data retaining the same relative functional "shape" while changing absolute magnitude. Of the two kinetic parameters, the activation barrier is the variable in the model that predominantly controls the shape of the extent of reaction versus exposure data. The above quoted uncertainty value for the activation barrier was obtained by performing the best-fit analysis described above to the extent of reaction data lying at both extremes of the error bars displayed in Figure 7. The activation barriers obtained when separately fitting the model to the data lying at each of the error bar extremes fell within the range of $8\ 500 \pm 500$ cal/mol. Another 200 cal/mol was added onto the quoted error value to account for random error fluctuations in the extent of reaction data points.

Finally, we wish to discuss the topic of MIR by comparing our results presented here to the results from the cyclobutane/Ru(001) MIR system. Recall that the MIR activation barrier and preexponential factor for cyclobutane on Ru(001) were determined to be $E_r = 7\ 510$ cal/mol and $k_r^{(0)} = 5 \times 10^{10}\ s^{-1}$, respectively. The identification of a C_4 metallacycle species on the surface immediately following MIR on Ru(001) implicated C−C bond cleavage as the initial reaction step described by these reported kinetic parameters. Similarly, the kinetic parameters for MIR reported above ($E_r = 8\ 500$ cal/mol and $k_r^{(0)} = 6.4 \times 10^{13}\ s^{-1}$) for the cyclobutane/Ir(111) MIR system are also thought to describe the dissociation of cyclobutane via initial C−C bond cleavage to form a C_4 metallacycle. Since these MIR kinetic parameters for both surfaces are thought to describe the same initial reaction step of cyclobutane ring-opening via C−C bond cleavage, it is not surprising that the activation barriers are quite similar. The lower activation barrier for MIR via C−C bond cleavage on Ru(001) compared to Ir(111) is not surprising in light of our very recent data[33] which show that the activation barrier for trapping-mediated dissocia-

tive chemisorption of cyclobutane via initial C−C bond cleavage is much lower on Ru(001) ($E_r = 10\,090$ cal/mol) than on Ir(111) ($E_r = 14\,750$ cal/mol).

Although the MIR activation barriers between the two surfaces were rather similar, the difference in preexponential factors between the two surfaces of 3 orders of magnitude is quite large. We believe that this large difference in preexponential factors can be explained qualitatively by the well-known compensation effect[34] in which a low preexponential factor usually accompanies a low activation barrier and a high preexponential factor usually accompanies a high activation barrier. Because of the compensation effect, we would expect that the higher activation barrier reported for Ir(111) compared to Ru(001) will lead to a higher preexponential on the Ir(111) surface, as is observed.

In the context of discussing MIR in a more general sense, an important point should be made regarding the previously mentioned comparisons between MIR activation barriers and those activation barriers measured for trapping-mediated reaction mechanisms at higher temperatures in the low coverage limit. When we first presented the topic of MIR for the cyclobutane/Ru(001) reaction system, it was proposed that MIR was simply a lowering of the activation barrier (due to the presence of a condensed multilayer) for the *same* initial reaction mechanism observed for trapping-mediated dissociative chemisorption in the low coverage limit. The data supported this initial hypothesis since C−C bond cleavage was found to be the initial dissociation step for trapping-mediated dissociative chemisorption[5] for the entire temperature range of 190 to 1200 K, and C−C bond cleavage was also found to be the initial dissociation step for MIR.[7] However, we have recently discovered that both initial C−C and C−H bond cleavage reactions occur in the trapping-mediated dissociative chemisorption of cyclobutane on Ir(111).[33] Initial C−C bond cleavage dominates at high temperatures ($E_r = 14\,750$ cal/mol), while initial C−H bond cleavage dominates at temperatures ($E_r = 10\,270$ cal/mol) as low as 300 K. Based on these measured activation barriers, trapping-mediated activation of cyclobutane on Ir(111) at cryogenic temperatures might be expected to occur via C−H bond cleavage. This most likely is not the case, however, since initial C−C bond cleavage is suggested as the initial MIR step for cyclobutane on Ir(111) based on the data presented for the experimental conditions studied here. These data obtained for the cyclobutane/Ir(111) reaction system allow us to conclude that MIR can occur via a different reaction mechanism than was observed for the trapping-mediated reaction. This observation raises our interest level in studying MIR systems on well-defined single-crystalline catalytic surfaces due to the potentially enormous impact that these studies can have in defining our understanding of heterogeneously catalyzed reactions that occur at the liquid−solid interface. These complementary trapping-mediated dissociative chemisorption and MIR studies of industrially important reaction systems may in the future serve as an invaluable method with which to determine the best operating conditions (e.g., gas−solid versus liquid−solid catalytic reaction system) at which to operate a reactor based on the desired product specifications.

As a final point of discussion, we would like to speculate on a mechanism for MIR of cyclobutane. Since C−C bond cleavage on transition-metal catalysts is often believed to involve metal electron donation into the C−C antibonding orbital,[35−37] we speculate that the presence of multilayer cyclobutane might contribute additional electron density into this antibonding orbital of the first layer cyclobutane, thus enhancing the rate of reaction in the presence of a multilayer. Molecular cyclobutane is expected to be a good electron donor due to the influence of ring strain on the electronic structure of the molecule; the electron density maxima of the C−C σ bonds lie outside the internuclear axis joining adjacent carbon atoms.[38] Therefore, if the second layer cyclobutane molecules are aligned such that the C−C σ bond electron density from the second-layer cyclobutane molecules overlaps with the C−C σ^* antibonding orbitals of the first-layer cyclobutane molecules, significant electron donation may occur, possibly providing an explanation for the MIR observed in the present work.

IV. Conclusions

The data presented here conclusively show that the multilayer-induced reaction of cyclobutane occurs on the Ir(111) surface. Whereas a monolayer coverage of cyclobutane desorbs essentially completely, reaction of cyclobutane adsorbates at the liquid−solid interface is significantly enhanced by the presence of condensed cyclobutane multilayers. Vibrational spectroscopic data collected prior to desorption of the β desorption product suggests the presence of an initial C_4H_8 metallacycle reaction intermediate. This observation implicates C−C bond cleavage as the initial reaction step in the MIR of cyclobutane on Ir(111). The TPD data collected under the experimental conditions studied here strongly suggest that the MIR of cyclobutane on Ir(111) results in the formation of three products: (1) desorption of *n*-butane, (2) desorption of 1-butene, and (3) dissociation to form surface carbon and hydrogen adatoms.

The extent of MIR has also been quantified and is used in conjunction with a kinetic model in order to quantify the kinetics of the MIR of cyclobutane on this surface. The MIR reaction kinetics are well described by a rate expression of the Polanyi−Wigner form with a preexponential factor of 6.4×10^{13} s^{-1} and an activation energy of $E_r = 8\,500 \pm 700$ cal/mol. The estimated error on the preexponential factor is plus-or-minus 1 order of magnitude. The activation barrier of 8 500 cal/mol measured here for MIR via initial C−C bond cleavage represents a significant decrease in the measured activation barrier for trapping-mediated dissociative chemisorption of cyclobutane at low temperature on Ir(111) via initial C−H bond cleavage of 10 270 cal/mol. The different initial reaction mechanisms observed for the MIR and trapping-mediated reaction of cyclobutane on Ir(111) suggest that the reaction proceeds via a different reaction mechanism depending on the whether the reaction occurs at the liquid−solid or the gas−solid interface.

Acknowledgment. This research was supported by the National Science Foundation under Grant No. CHE-9981769 and the Department of Energy under Grant No. DE-FG03-89ER14048. C.H. and M.W. also received support from the NSF predoctoral fellowship program. Special thanks to Peter Mikesell and Professor Daniel Little for the synthesis of cyclobutane.

References and Notes

(1) Madix, R. J.; Roberts, J. T. *Surface Reactions*; Springer-Verlag: Berlin, 1994.
(2) Zaera, F. *Chem. Rev.* **1995**, *95*, 2651.
(3) Bent, B. E. *Chem. Rev.* **1996**, *96*, 1361.
(4) Hagedorn, C. J.; Weiss, M. J.; Weinberg, W. H. *J. Am. Chem. Soc.* **1998**, *120*, 11824.
(5) Hagedorn, C. J.; Weiss, M. J.; Chung, C.-H.; Mikesell, P. J.; Little, R. D.; Weinberg, W. H. *J. Chem. Phys.* **1999**, *110*, 1745.
(6) Johnson, D. F.; Weinberg, W. H. *J. Chem. Phys.* **1994**, *101*, 6289.
(7) Weiss, M. J.; Hagedorn, C. J.; Mikesell, P. J.; Little, R. D.; Weinberg, W. H. *J. Am. Chem. Soc.* **1998**, *110*, 11812.
(8) Weiss, M. J.; Hagedorn, C. J.; Weinberg, W. H. *J. Am. Chem. Soc.* **1999**, *121*, 5047.

(9) Weiss, M. J.; Hagedorn, C. J.; Weinberg, W. H. *Surf. Sci.* **1999**, *426*, 154.
(10) Weiss, M. J.; Hagedorn, C. J.; Weinberg, W. H. *J. Vac. Sci. Technol. A* **1998**, *16*, 3521.
(11) Taylor, J. L.; Ibbotson, D. E.; Weinberg, W. H. *J. Chem. Phys.* **1978**, *69*, 4298.
(12) Engstrom, J. R.; Weinberg, W. H. *Rev. Sci. Instrum.* **1984**, *55*, 404.
(13) Hagedorn, C. J.; Weiss, M. J.; Weinberg, W. H. *J. Vac. Sci. Technol. A*, in press.
(14) Connor, D. S.; Wilson, E. R. *Tetrahedron Lett.* **1967**, *49*, 4925.
(15) Schick, M.; Lauterbach, J.; Weinberg, W. H. *J. Vac. Sci. Technol. A* **1996**, *14*, 1448.
(16) Redhead, P. A. *Vacuum* **1962**, *12*, 203.
(17) *Index of Mass Spectral Data*; American Society for Testing and Materials: Philadelphia, 1969.
(18) Engstrom, J. R.; Goodman, D. W.; Weinberg, W. H. *J. Vac. Sci. Technol. A* **1987**, *5*, 825.
(19) Engstrom, J. R.; Goodman, D. W.; Weinberg, W. H. *J. Phys. Chem.* **1990**, *94*, 396.
(20) Szuromi, P. D.; Engstrom, J. R.; Weinberg, W. H. *J. Chem. Phys.* **1984**, *80*, 508.
(21) Wittrig, T. S.; Szuromi, P. D.; Weinberg, W. H. *J. Chem. Phys.* **1982**, *76*, 3305.
(22) Marinova, T. S.; Chakarov, D. V. *Surf. Sci.* **1988**, *200*, 309.
(23) Marinova T. S.; Chakarov, D. V. *Surf. Sci.* **1987**, *192*, 275.
(24) Nakao, F. *Vacuum* **1975**, *25*, 431.
(25) Madix, R. J. *Surf. Sci.* **1994**, *300*, 785.
(26) Johnson, D. F.; Weinberg, W. H. *J. Chem. Phys.* **1995**, *103*, 5833.
(27) Gatial, A.; Klaeboe, P.; Nielsen, C. J.; Powell, D. L.; Sülzle, D.; Kondow, A. J. *Raman Spectrosc.* **1989**, *20*, 239.
(28) *NIST Chemistry WebBook*: http://webbook.nist.gov.
(29) Thiel, P. A.; Madey, T. E. *Surf. Sci. Rep.* **1987**, *7*, 211.
(30) Marinova, T. S.; Chakarov, D. V. *Surf. Sci.* **1989**, *217*, 65.
(31) Hagedorn, C. J.; Weiss, M. J.; Weinberg, W. H. *Phys. Rev. B* **1999**, *60*, R14016.
(32) Lauterbach, J.; Schick, M.; Weinberg, W. H. *J. Vac. Sci. Technol. A* **1996**, *14*, 1511.
(33) Hagedorn, C. J.; Weiss, M. J.; Kim, T. W.; Weinberg, W. H. *J. Am. Chem. Soc.*, in preparation.
(34) Christmann, K. *Surface Physical Chemistry*; Steinkopff: Darmstadt, Germany, 1991.
(35) Sault, A. G.; Goodman, D. W. *J. Chem. Phys.* **1988**, *88*, 7232.
(36) Siegbahn, P. E. M.; Blomberg, M. R. A. *J. Am. Chem. Soc.* **1992**, *114*, 10548.
(37) Crabtree, R. H. *Chem. Rev.* **1985**, *85*, 245.
(38) Stein, A.; Lehmann, C. W.; Luger, P. *J. Am. Chem. Soc.* **1992**, *114*, 7684.
(39) Barnes, A. J.; Hallam, H. E.; Howells, J. D. R.; Scrimshaw, G. F. *J. Chem. Soc., Faraday II* **1973**, *69*, 738.
(40) Crowder, G. A.; Ali, S. *J. Mol. Struct.* **1975**, *25*, 377.
(41) *Standard Infrared Grating Spectra*; The Sadtler Company: Philadelphia, 1985.
(42) Gallinella, E.; Cadioli, B. *Vib. Spectrosc.* **1997**, *13*, 163.